Dynamics of shock waves in elastic-plastic solids

Nicolas Favrie, Sergey L. Gavrilyuk

Dynamics of shock waves in elastic-plastic solids

N. Favrie*and S. Gavrilyuk†

Abstract

The Maxwell type elastic-plastic solids are characterized by decaying the absolute values of the principal components of the deviatoric part of the stress tensor during the plastic relaxation step. We propose a mathematical formulation of such a model which is compatible with the von Mises criterion of plasticity. Numerical examples show the ability of the model to deal with complex physical phenomena.

Key words : elastic-plastic solids, large deformations, Godunov type methods

1 Introduction

There is a lack of a generally accepted formulation for finite deformation elasto-plasticity capable to describe shock wave propagation in solids. "Although the term plastic deformation seems to be rather customary in engineering, it turns out in the context of large deformations that it is extremely difficult to define it precisely" (Bertram, 2005). A class of hyperbolic type models describing the plastic behavior of materials under large stresses has been proposed by Godunov (1978) and Godunov and Romenskii (2003). We have proposed an extension of such a model to situations not necessarily involving large stresses (Favrie and Gavrilyuk, 2010). The model verifies some experimentally observed facts usually occurring during plastic deformations :

- The density does not evolve during the plastic relaxation process
- Entropy is created when plasticity occurs (irreversibility of plastic deformations)
- The intensity of shear stresses decreases (Maxwell type model)
- The von Mises yield limit is reached at the end of relaxation process

This paper is organized as follows. In Section 2, we remind the model derived in Favrie and Gavrilyuk (2010). Section 3 details the numerical method to solve this model. In particular, a splitting method is used to describe an elastic (hyperbolic) step and a step corresponding to plastic deformations (relaxation). One-dimensional dynamics and quasistatic tests are presented in Section 4. Finally, we present the perspectives in applying such a model to fluid-structure interaction problems.

2 Governing equations of elastic-plastic solids

The governing equations of *elastic-plastic* solids describing the behavior of materials under large stresses (or, what is equivalent, for small values of the yield strength) were proposed, in particular, in Godunov (1978), Miller and Colella (2001), Godunov and Romenskii (2003), Godunov and Peshkov (2010) and Barton *et al.* (2010). We take them in the following generic form permitting

*Université d'Aix-Marseille & C.N.R.S. U.M.R. 6595, IUSTI, Project SMASH, 5 rue E. Fermi, 13453 Marseille Cedex 13 France, nicolas.favrie@polytech.univ-mrs.fr

†Corresponding author, Université d'Aix-Marseille & C.N.R.S. U.M.R. 6595, IUSTI, Project SMASH, 5 rue E. Fermi, 13453 Marseille Cedex 13 France, sergey.gavrilyuk@polytech.univ-mrs.fr

their generalization to plastic deformations for finite values of the yield strength (Favrie and Gavrilyuk, 2010):

$$\begin{aligned}
&\frac{D}{Dt}\mathbf{e}^{\beta}+\left(\frac{\partial \mathbf{v}}{\partial \mathbf{x}}\right)^{T}\mathbf{e}^{\beta}=-\frac{1}{\tau_{rel}}\mathbf{R}\mathbf{e}^{\beta}, \quad \frac{D}{Dt}=\frac{\partial}{\partial t}+\mathbf{v}\cdot\nabla,\\
&\frac{\partial \rho}{\partial t}+\operatorname{div}(\rho\mathbf{v})=0,\\
&\frac{\partial \rho\mathbf{v}}{\partial t}+\operatorname{div}(\rho\mathbf{v}\otimes\mathbf{v}-\sigma)=0,\\
&\frac{\partial(\rho E)}{\partial t}+\operatorname{div}(\rho\mathbf{v}E-\sigma\mathbf{v})=0,
\end{aligned} \tag{1}$$

Here $\mathbf{e}^{\beta}$ is the *elastic local cobasis*. In general, it is not rotation free as it occurs for elastic solids where such vectors are gradients of the Lagrangian coordinates (see Gavrilyuk *et al.*, 2008). Also, we define the *elastic Finger tensor* $\mathbf{G}=\sum_{\beta=1}^{3}\mathbf{e}^{\beta}\otimes\mathbf{e}^{\beta}$ (it is also called *effective elastic deformation tensor* by Godunov (1978) and Godunov and Romenskii (2003)), and the *elastic deformation gradient* $\mathbf{F}$ related to $\mathbf{e}^{\beta}$ through : $\mathbf{F}^{-T}=\left(\mathbf{e}^{1},\mathbf{e}^{2},\mathbf{e}^{3}\right)$. $\rho=\rho_0\left|\mathbf{G}\right|^{1/2}$ is the solid density, ρ_0 is the reference density depending only on the Lagrangian coordinates, $\mathbf{v}$ is the velocity field, σ is the stress tensor, $E=e+\frac{1}{2}\left|\mathbf{v}\right|^{2}$ is the specific total energy, $e\left(\mathbf{G},\eta\right)$ is the specific internal energy depending only on invariants of $\mathbf{G}$, η is the specific entropy. The symmetric stress tensor is given by :

$$\sigma=-2\rho\frac{\partial e}{\partial \mathbf{G}}\mathbf{G}=-p\mathbf{I}+\mathbf{S}, \qquad tr(\mathbf{S})=\mathbf{0},$$

where p is the hydrodynamic pressure, and $\mathbf{S}$ is the deviatoric part of the stress tensor. Such a model should be closed by giving the equation of state $e\left(\mathbf{G},\eta\right)$. We take the energy in separate form :

$$e=\varepsilon^{h}\left(\rho,\eta\right)+\varepsilon^{e}(\mathbf{g}) \tag{2}$$

where

$$\mathbf{g}=\frac{\mathbf{G}}{\left|\mathbf{G}\right|^{1/3}}.$$

The elastic part of the internal energy $\varepsilon^{e}(\mathbf{g})$ depends only on $\mathbf{g}$. The tensor $\mathbf{g}$ has a unit determinant, so it is unaffected by the volume change. The idea to take the arguments of the internal energy in the form ρ, η and $\mathbf{g}$ was proposed, in particular, in Gouin and Debieve (1986) (see also Simo and Hughes (1998), Plohr and Plohr (2005)), but for the dependence of the energy on the right Cauchy-Green tensor $\mathbf{C}=\mathbf{F}^{T}\mathbf{F}$. However, the choice of the Finger tensor is more natural for the Eulerian description of solids. The stress tensor is then

$$\sigma=-2\rho\frac{\partial e}{\partial \mathbf{G}}\mathbf{G}=-p\mathbf{I}+\mathbf{S}, \qquad tr\left(\mathbf{S}\right)=0,$$

where the thermodynamic pressure is :

$$p=\rho^{2}\frac{\partial \varepsilon^{h}}{\partial \rho}.$$

The shear part of the energy has no influence on the pressure, it is determined only by the hydrodynamic part. A particular form of the energy taken for applications is as follows. The hydrodynamic part of the energy $\varepsilon^{h}\left(\rho,s\right)$ is taken in the form of stiffened gas EOS :

$$\varepsilon^{h}\left(\rho,p\right)=\frac{p+\gamma p_{\infty}}{\rho\left(\gamma-1\right)}, \quad p+p_{\infty}=A\exp\left(\frac{\eta-\eta_0}{c_v}\right)\rho^{\gamma}, \quad \eta_0=const, \quad A=const, \tag{3}$$

and the elastic energy $\varepsilon^e(\mathbf{g})$ is :

$$\varepsilon^e(\mathbf{g}) = \frac{\mu}{4\rho_0} tr\left((\mathbf{g}-\mathbf{I})^2\right) = \frac{\mu}{4\rho_0}\left(\frac{J_2}{\left|\hat{\mathbf{G}}\right|^{2/3}} - \frac{2J_1}{\left|\hat{\mathbf{G}}\right|^{1/3}} + 3\right), \qquad J_i = tr\left(\mathbf{G}^i\right), \qquad i = 1,2, \quad (4)$$

where μ is the shear modulus. The choice (3)-(4) guarantees, in particular, the hyperbolicity of (1) (Favrie *et al.* (2009)) and hence the well-posedness of the corresponding Cauchy problem. The stress tensor will be then

$$\sigma = -2\rho\frac{\partial e}{\partial \mathbf{G}}\mathbf{G} = -p\mathbf{I}+\mathbf{S}, \qquad \mathbf{S} = -\mu\frac{\rho}{\rho_0}\left(\frac{1}{|\mathbf{G}|^{2/3}}\left(\mathbf{G}^2 - \frac{J_2}{3}\mathbf{I}\right) - \frac{1}{|\mathbf{G}|^{1/3}}\left(\mathbf{G} - \frac{J_1}{3}\mathbf{I}\right)\right), \qquad tr\left(\mathbf{S}\right) = 0, \quad (5)$$

The *real Finger tensor* $\hat{\mathbf{G}}$ is obtained in the following way. We calculate the trajectories of the solid body :

$$\frac{d\mathbf{x}}{dt} = \mathbf{v},$$
$$\mathbf{x}|_{t=0} = \mathbf{X},$$

where $\mathbf{X}$ are the Lagrangian coordinates. Then we calculate the real deformation gradient

$$\hat{\mathbf{F}} = \frac{\partial \mathbf{x}}{\partial \mathbf{X}}$$

and finally the real Finger tensor :

$$\hat{\mathbf{G}} = \left(\hat{\mathbf{F}}^T\right)^{-1}\hat{\mathbf{F}}^{-1}.$$

The real Finger tensor verifies the equation

$$\frac{D\hat{\mathbf{G}}}{Dt} + \hat{\mathbf{G}}\frac{\partial \mathbf{v}}{\partial \mathbf{x}} + \left(\frac{\partial \mathbf{v}}{\partial \mathbf{x}}\right)^T\hat{\mathbf{G}} = 0. \quad (6)$$

The evolution equation for the elastic Finger tensor $\mathbf{G} = \sum_{\beta=1}^{3} \mathbf{e}^\beta \otimes \mathbf{e}^\beta$ is :

$$\frac{D\mathbf{G}}{Dt} + \left(\frac{\partial \mathbf{v}}{\partial \mathbf{x}}\right)^T\mathbf{G} + \mathbf{G}\frac{\partial \mathbf{v}}{\partial \mathbf{x}} = -\frac{1}{\tau_{rel}}\left(\mathbf{GR}+\mathbf{RG}\right). \quad (7)$$

To close this generic system (1) the relaxation term $\mathbf{R}$ and the relaxation time $\tau_{rel} > 0$ should be determined in such a way that :

- They should be compatible with the mass conservation law
- They should be compatible with the entropy inequality
- The intensity of shear stresses decays during the relaxation (Maxwell type model)
- They should be compatible with the von Mises yield criterion

  To satisfy the first two conditions it is sufficient to choose $\mathbf{R}$ in the form

  $$\mathbf{R} = -a\mathbf{S}$$

  where a is a positive scalar function : $a > 0$. However, the two last conditions are more delicate. We will repeat here the arguments given in Favrie and Gavrilyuk (2010).

2.1 Compatibility with the von Mises criterion of yielding

Consider the *yield function*

$$f(\mathbf{S}) = \mathbf{S} : \mathbf{S} - \frac{2}{3}Y^2.$$

The surface $f(\mathbf{S}) = 0$ is *yield surface*, Y is the *yield strength*. According to the von Mises criterion of yielding, if the yield function is negative, the material is elastic, while in opposite case we have a plastic behaviour.

Consider the *singular value decomposition* of $\mathbf{F}^{-1}$: $\mathbf{F}^{-1} = \mathbf{UKV}^T$, where $\mathbf{U}$ and $\mathbf{V}$ are orthogonal matrices and $\mathbf{K}$ is the diagonal matrix (see, for example, Godunov and Romenskii, 2003). The eigenvalues κ_α of the matrix $\mathbf{G} = \mathbf{F}^{-T}\ \mathbf{F}^{-1}$ are related to the eigenvalues k_α of the diagonal matrix $\mathbf{K}$ (or, what is the same, the singular values of $\left(\mathbf{F}^T\right)^{-1}$) by

$$\kappa_\alpha = k_\alpha^2$$

Let us suppose that the matrices $\mathbf{U}$ and $\mathbf{V}$ do not vary during the relaxation process. This hypothesis was proposed in Godunov (1978), Godunov and Romenskii (2003) and Godunov and Peshkov (2010). It is related to the fact that the description of the Maxwell-like models in terms of deformation is not direct. So, we have to decompose the relaxation process into two parts. One of them is related to the geometry through the orthogonal matrices $\mathbf{U}$ and $\mathbf{V}$, and other one to the physics through the eigenvalues of $\mathbf{K}$ (or $\mathbf{G}$). The geometry varies only if the elastic deformations occur, while it is "frozen" during the relaxation process. Since we know at the end of the relaxation process the eigenvalues κ_α (or k_α), we can easily reconstruct the local cobasis $\mathbf{e}^\alpha$ since the matrices $\mathbf{U}$ and $\mathbf{V}$ are unchanged. The reconstructed local cobasis is not necessarily rotation free. If space variations do not occur during the relaxation process, the derivative $\frac{D}{Dt}$ should be replaced by the partial derivative with respect to time :

$$\frac{D}{Dt} = \frac{\partial}{\partial t},$$

and we will simply write

$$\frac{\partial}{\partial t} = \frac{d}{dt}.$$

This relaxation procedure comes from the numerical treatment of the problem which will be discussed in detail in Section 3. For each numerical cell, we want to solve the following relaxation equation :

$$\frac{d\mathbf{G}}{dt} = -\frac{1}{\tau_{rel}}(\mathbf{GR} + \mathbf{RG}) = \frac{a}{\tau_{rel}}(\mathbf{GS} + \mathbf{SG}) = \frac{2a}{\tau_{rel}}(\mathbf{GS}) \tag{8}$$

since in the isotropic case the tensor $\mathbf{GS}$ is symmetric. Or, in terms of eigenvalues of $\mathbf{G}$:

$$\frac{d\kappa_\alpha}{dt} = \frac{2a}{\tau_{rel}}\kappa_\alpha S_\alpha \tag{9}$$

Obviously, equations (9) (or, equivalently, (8)) admit the first integral which is just the mass conservation law :

$$\frac{d(\kappa_1\kappa_2\kappa_3)}{dt} = 0.$$

The fact that the density conserves during plastic deformations is quite conventional (Germain and Lee (1973), Godunov (1978)). We will denote

$$\kappa_1\kappa_2\kappa_3 = \omega = \left(\frac{\rho}{\rho_0}\right)^2 = const.$$

We introduce new variables

$$\beta_\alpha = \frac{\kappa_\alpha}{(\kappa_1\kappa_2\kappa_3)^{1/3}}$$

In these variables the relaxation equations are

$$\frac{d\beta_\alpha}{dt} = \frac{2a}{\tau_{rel}}\beta_\alpha S_\alpha, \tag{10}$$

where

$$S_\alpha = -\mu\omega^{1/2}\left(\beta_\alpha^2 - \beta_\alpha - \frac{\beta_1^2 - \beta_1 + \beta_2^2 - \beta_2 + \beta_3^2 - \beta_3}{3}\right) \tag{11}$$

$$= -\mu\omega^{1/2}\left(\left(\beta_\alpha - \frac{1}{2}\right)^2 - \frac{\left(\beta_1 - \frac{1}{2}\right)^2 + \left(\beta_2 - \frac{1}{2}\right)^2 + \left(\beta_3 - \frac{1}{2}\right)^2}{3}\right).$$

Let us show that

$$L = \mathbf{S} : \mathbf{S}.$$

is a Lyapounov function, i.e. its time derivative is negative. Replacing (11) we have :

$$L = \sum_\alpha S_\alpha^2 = \mu^2\omega\left(\sum_\alpha\left(\beta_\alpha - \frac{1}{2}\right)^4 - \frac{1}{3}\left(\sum_\alpha\left(\beta_\alpha - \frac{1}{2}\right)^2\right)^2\right).$$

Differentiating it with respect to time we obtain :

$$\frac{dL}{dt} = \frac{d}{dt}\left(\sum_\alpha S_\alpha^2\right) = \mu^2\omega\frac{d}{dt}\left(\sum_\alpha\left(\beta_\alpha - \frac{1}{2}\right)^4 - \frac{1}{3}\left(\sum_\alpha\left(\beta_\alpha - \frac{1}{2}\right)^2\right)^2\right)$$

$$= 4\mu^2\omega\left(\sum_\alpha\left(\beta_\alpha - \frac{1}{2}\right)^3\frac{d\beta_\alpha}{dt} - \frac{1}{3}\left(\sum_\gamma\left(\beta_\gamma - \frac{1}{2}\right)^2\right)\sum_\alpha\left(\beta_\alpha - \frac{1}{2}\right)\frac{D\beta_\alpha}{Dt}\right)$$

$$= 4\mu^2\omega\left(\sum_\alpha\left(\beta_\alpha - \frac{1}{2}\right)\frac{d\beta_\alpha}{dt}\left(\left(\beta_\alpha - \frac{1}{2}\right)^2 - \frac{1}{3}\sum_\gamma\left(\beta_\gamma - \frac{1}{2}\right)^2\right)\right)$$

$$= 4\mu^2\omega\left(\sum_\alpha\left(\beta_\alpha - \frac{1}{2}\right)\frac{d\beta_\alpha}{dt}\left(\left(\beta_\alpha - \frac{1}{2}\right)^2 - \frac{1}{3}\sum_\gamma\left(\beta_\gamma - \frac{1}{2}\right)^2\right)\right)$$

$$= -8\mu\omega^{1/2}\frac{a}{\tau_{rel}}\sum_\alpha\beta_\alpha\left(\beta_\alpha - \frac{1}{2}\right)S_\alpha^2. \tag{12}$$

The inequality

$$\frac{dL}{dt} < 0$$

is obviously true in the vicinity of the equilibrium where all $\beta_\alpha = 1$. However, this result is not only local. A numerical study shows that the right hand side of (12) is negative for any $\beta_\alpha > 0$ such that $\beta_1\beta_2\ \beta_3 = 1$. Hence, L is a Lyapounov function for (10).

Since only the ratio a/τ_{rel} is important, we choose a as

$$2a = \frac{1}{\mu\omega^{1/2}}$$

and the relaxation time in the form :

$$\frac{1}{\tau_{rel}} = \begin{cases} \frac{1}{\tau_0}\left(\frac{\sum_\alpha S_\alpha^2 - \frac{2}{3}Y^2}{\mu^2}\right)^n, \text{if } \sum_\alpha S_\alpha^2 - \frac{2}{3}Y^2 > 0 \\ 0\ , \text{if } \sum_\alpha S_\alpha^2 - \frac{2}{3}Y^2 \le 0 \end{cases}, \tag{13}$$

where τ_0 is a characteristic constant time, and $n > 0$. Inequality (12) shows, in particular, that with such a choice of the relaxation time the trajectories are attracted to the yield surface in finite time if $1 > n > 0$, and in infinite time if $n \geq 1$.

In severe conditions the deviatoric part of the stress tensor can be neglected and one can put $Y = 0$. For such a limit situation different formulas for the relaxation time can be found in Godunov *et al.* (1975).

Finally, the governing equations in terms of β_α are :

$$\frac{d\beta_\alpha}{dt} = -\frac{\beta_\alpha}{\tau_{rel}}\left(\left(\beta_\alpha - \frac{1}{2}\right)^2 - \frac{\left(\beta_1 - \frac{1}{2}\right)^2 + \left(\beta_2 - \frac{1}{2}\right)^2 + \left(\beta_3 - \frac{1}{2}\right)^2}{3}\right) \tag{14}$$

Even if the ordinary differential equations for β_α can easily be solved numerically, it would be useful to have simple algebraic relations (exact solutions) of the time dependence of β_α, to make numerical codes more efficient. Here we present such a simplification in the case of small deformations. Let $\beta_\alpha = 1 + \gamma_\alpha$ where γ_α is small. We can estimate now the principal eigenvalues of the deviatoric part of the stress tensor :

$$S_\alpha = -\mu\omega^{1/2}\left(\beta_\alpha^2 - \beta_\alpha - \frac{\beta_1^2 - \beta_1 + \beta_2^2 - \beta_2 + \beta_3^2 - \beta_3}{3}\right) = -\mu\omega^{1/2}\gamma_\alpha + O\left(\gamma_\alpha^2\right)$$

The equations (14) can be replaced by the approximate ones :

$$\frac{d\gamma_\alpha}{dt} = -\frac{\gamma_\alpha}{\tau_{rel}}.$$

Or, equivalently,

$$\frac{dS_\alpha}{dt} = -\frac{S_\alpha}{\tau_{rel}}. \tag{15}$$

However, we will not suppose that the relaxation time is constant. We will choose it, for example, in the form :

$$\frac{1}{\tau_{rel}} = \frac{1}{\tau_0}\left(\frac{\sum_\alpha S_\alpha^2 - \frac{2}{3}Y^2}{\mu^2}\right) = \frac{1}{\tau_0}\left(\sum_\alpha \frac{S_\alpha^2}{\mu^2} - \xi^2\right), \quad \tau_0 = const, \quad \xi^2 = \frac{2}{3}\frac{Y^2}{\mu^2}. \tag{16}$$

Then (15), (16) admit a time dependent first integral :

$$\sum_\alpha \frac{S_\alpha^2}{\mu^2} = \frac{\xi^2 \sum_\alpha \frac{S_\alpha^2|_{t=0}}{\mu^2}}{\sum_\alpha \frac{S_\alpha^2|_{t=0}}{\mu^2} + \left(\xi^2 - \sum_\alpha \frac{S_\alpha^2|_{t=0}}{\mu^2}\right)\exp\left(-2\xi^2 t/\tau_0\right)}.$$

It gives an explicit expression for the relaxation time :

$$\frac{1}{\tau_{rel}} = \frac{1}{\tau_0}\left(\sum_\alpha \frac{S_\alpha^2}{\mu^2} - \xi^2\right) =$$

$$\frac{1}{\tau_0}\left(\frac{\xi^2\left(\sum_\alpha \frac{S_\alpha^2|_{t=0}}{\mu^2} - \xi^2\right)\exp\left(-2\xi^2 t/\tau_0\right)}{\sum_\alpha \frac{S_\alpha^2|_{t=0}}{\mu^2} + \left(\xi^2 - \sum_\alpha \frac{S_\alpha^2|_{t=0}}{\mu^2}\right)\exp\left(-2\xi^2 t/\tau_0\right)}\right) = \frac{1}{\tau_0}\left(\frac{\xi^2\left(\sum_\alpha \frac{S_\alpha^2|_{t=0}}{\mu^2} - \xi^2\right)}{\sum_\alpha \frac{S_\alpha^2|_{t=0}}{\mu^2}\exp\left(2\xi^2 t/\tau_0\right) + \left(\xi^2 - \sum_\alpha \frac{S_\alpha^2|_{t=0}}{\mu^2}\right)}\right) =$$

$$\frac{\xi^2}{\tau_0}\left(\frac{1}{\frac{\sum_\alpha \frac{S_\alpha^2|_{t=0}}{\mu^2}}{\left(\sum_\alpha \frac{S_\alpha^2|_{t=0}}{\mu^2} - \xi^2\right)}\exp\left(2\xi^2 t/\tau_0\right) - 1}\right) = \frac{\xi^2}{\tau_0}\frac{1}{C_0\exp\left(2\xi^2 t/\tau_0\right) - 1}$$

where

$$C_0 = \frac{\sum\limits_\alpha \frac{S_\alpha^2|_{t=0}}{\mu^2}}{\sum\limits_\alpha \frac{S_\alpha^2|_{t=0}}{\mu^2} - \xi^2} > 1$$

Then, the equations for S_α (15) become linear :

$$\frac{dS_\alpha}{dt} = -\frac{\xi^2 S_\alpha}{\tau_0} \frac{1}{C_0 \exp\left(2\xi^2 t/\tau_0\right) - 1}.$$

The solution of these equations is :

$$S_\alpha = \sqrt{C_0 - 1}\; S_\alpha|_{t=0} \frac{e^{\xi^2 t/\tau_0}}{\sqrt{C_0 e^{2\xi^2 t/\tau_0} - 1}}. \tag{17}$$

This explicit formula reflects quite well the qualitative behavior of the deviatoric part of the stress tensor. In particular, if the characteristic scale Δt is large with respect to the relaxation scale τ_0, the final values of S_α can be estimated as :

$$S_{\alpha f} \approx \frac{\sqrt{C_0 - 1}}{\sqrt{C_0}}\; S_\alpha|_{t=0}\,.$$

Obviously,

$$\sum_\alpha S_{\alpha f}^2 = \frac{C_0 - 1}{C_0} \sum_\alpha S_\alpha^2|_{t=0} = \mu^2 \xi^2 = \frac{2}{3} Y^2.$$

This asymptotic result can be used for the construction of efficient Riemann solvers in the case where the temporal time step is much larger than characteristic relaxation time.

3 Numerical method

The aim of this section is to derive a Godunov type method with an approximate Riemann solver. This model is solved in two steps which are detailed below.

3.1 Hyperbolic step

First, we compute the elastic part of the model. The model is equivalent to the following one written in terms of cobasis vectors $\mathbf{e}^\alpha$

$$\frac{D\mathbf{e}^\alpha}{Dt} + \left(\frac{\partial \mathbf{v}}{\partial \mathbf{x}}\right)^T \mathbf{e}^\alpha = 0,$$

$$\frac{\partial \rho}{\partial t} + \operatorname{div}(\rho \mathbf{v}) = 0,$$

$$\frac{\partial \rho \mathbf{v}}{\partial t} + \operatorname{div}(\rho \mathbf{v} \otimes \mathbf{v} - \sigma) = 0,$$

$$\frac{\partial \rho E}{\partial t} + \operatorname{div}(\rho E \mathbf{v} - \sigma \mathbf{v}) = 0.$$

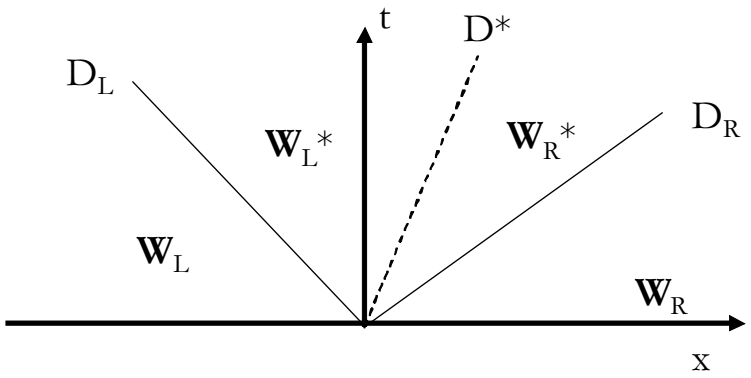

Figure 1: An approximate solution of the Riemman problem.

3.1.1 HLLC Riemann solver

This solver considers each wave as a discontinuity (see Figure 1). In the HLLC framework only two extremes waves and the contact discontinuity are considered.

Jump relations for physical variables:

Each wave being considered as a discontinuity and the system being conservative, the Rankine-Hugoniot relations across each limit wave (D_L, D_R, D^*) read :

$$\mathbf{H}_L^* - D_L \mathbf{W}_L^* = \mathbf{H}_L - D_L \mathbf{W}_L$$

$$\mathbf{H}_R^* - D_R \mathbf{W}_R^* = \mathbf{H}_R - D_R \mathbf{W}_R$$

$$\mathbf{H}_R^* - D^* \mathbf{W}_R^* = \mathbf{H}_L^* - D^* \mathbf{W}_L^*$$

where $\mathbf{W} = (\rho, \rho u, \rho v, \rho E)^T$ is the vector of unknowns, and $\mathbf{H} = \left(\rho u, \rho u^2 - \sigma_{11}, \rho uv - \sigma_{12}, \rho uE - \sigma_{11} u - \sigma_{12} v\right)^T$ is the flux vector. The meaning of indices is shown in Figure 1.

Jump relations for geometrical variables:

The geometrical equations are :

$$\frac{\partial a^\alpha}{\partial t} + \frac{\partial a^\alpha u}{\partial x} + b^\alpha \frac{\partial v}{\partial x} = 0, \tag{18}$$

$$\frac{\partial b^\alpha}{\partial t} + u \frac{\partial b^\alpha}{\partial x} = 0,$$

$$\frac{\partial c^\alpha}{\partial t} + u \frac{\partial c^\alpha}{\partial x} = 0.$$

Here a^α, b^α and c^α are the components of the vector $\mathbf{e}^\alpha$. It follows that we have the following invariants across left- and-right-facing waves (see Figure 1):

$$b^\alpha = (b^\alpha)_0 \, , c^\alpha = (c^\alpha)_0 \, .$$

Here the index "0" runs "L" or "R". Thus there is no difficulty to determine jump relation for the a^αvariables :

$$a^\alpha (u - D) + b^\alpha v = (a^\alpha (u - D) + b^\alpha v)_0$$

Interface relations

The equations (18) show that if the term b^α is non zero at the contact discontinuities then necessarily the tangential velocity should be continuous, $[v] = 0$. If not, the non conservative product is not well defined. Thus, the resulting set of interface relations is :

$$[v] = 0, [u] = 0, [\sigma_{11}] = 0, [\sigma_{12}] = 0$$

The limit wave speeds are approximated by Davis estimates (1988) :

$$D_R = \max\left(u_L + c_L, u_R + c_R\right)$$

$$D_L = \min\left(u_L - c_L, u_R - c_R\right)$$

where $c_{R,L}$are the longitudinal sound speeds of the material. The speed of the intermediate wave (or contact discontinuity) is estimate under HLL approximation:

$$u^* = D^* = \frac{\left(\rho u^2 - \sigma_{11}\right)_L - \left(\rho u^2 - \sigma_{11}\right)_R - D_L\left(\rho u\right)_L + D_R\left(\rho u\right)_R}{\left(\rho u\right)_L - \left(\rho u\right)_R - D_L\rho_L + D_R\rho_R}$$

From these wave speeds, the conservative state variables in the star region are determined:

$$\left(\rho\right)_L^* = \left(\rho\right)_L \frac{D_L - u_L}{D_L - D^*},$$

$$\sigma_{11R}^* = \sigma_{11R} - \rho_R u_R\left(u_R - D_R\right) + \rho_R^* D^*\left(D^* - D_R\right), \qquad \sigma_{11L}^* = \sigma_{11L} - \rho_L u_L\left(u_L - D_L\right) + \rho_L^* D^*\left(D^* - D_L\right),$$

$$\left(\sigma_{12}\right)^* = \frac{\left(u_R - D_R\right)\rho_R\left(\sigma_{12}\right)_L - \left(u_L - D_L\right)\rho_L\left(\sigma_{12}\right)_R + \left(u_L - D_L\right)\rho_L\left(u_R - D_R\right)\rho_R\left(v_R - v_L\right)}{\left(\left(u_R - D_R\right)\rho_R - \left(u_L - D_L\right)\rho_L\right)}$$

$$v_L^* = v_L + \frac{\left(\sigma_{12}\right)^* - \left(\sigma_{12}\right)_L}{\left(u^* - D_L\right)\rho_L}$$

$$v_R^* = v_R + \frac{\left(\sigma_{12}\right)^* - \left(\sigma_{12s}\right)_R}{\left(u_R - D_R\right)\rho_R}$$

$$\left(a_L^2\right)^* = \frac{a_L^2\left(u^* - D_L\right) + b_L^2\left(v_L - v_L^*\right)}{\left(u^* - D_L\right)} \text{ and } \left(a_R^2\right)^* = \frac{a_R^2\left(u^* - D_R\right) + b_R^2\left(v_R - v_R^*\right)}{\left(u^* - D_R\right)}$$

$$\left(a_L^1\right)^* = \frac{a_L^1\left(u^* - D_L\right) + b_L^1\left(v_L - v^*\right)}{\left(u^* - D_L\right)} \text{ and } \left(a_R^1\right)^* = \frac{a_R^1\left(u^* - D_R\right) + b_R^1\left(v_R - v_R^*\right)}{\left(u^* - D_R\right)}$$

$$b_L^{2*} = b_L^2 \text{ and } b_R^{2*} = b_R^2$$
$$b_L^{1*} = b_L^1 \text{ and } b_R^{1*} = b_R^1$$
$$c_L^{3*} = c_L^3 \text{ and } c_R^{3*} = c_R^3$$

$$E_R^* = \frac{\rho_R E_R(u_R - D_R) - \sigma_{11R}u_R - \sigma_{12R}v_R + \sigma_{11R}^* D^* + \sigma_{12R}^* v^*}{\rho_R^*(D^* - D_R)}$$

$$E_L^* = \frac{\rho_L E_L(u_{_R} - D_L) - \sigma_{11L}u_L - \sigma_{12L}v_L + \sigma_{11L}^* D^* + \sigma_{12L}^* v^*}{\rho_L^*(D^* - D_L)},$$

with

$$E = \varepsilon^h\left(\rho, \eta\right) + \varepsilon^e(\mathbf{g}) + \frac{1}{2}u^2 + \frac{1}{2}v^2.$$

3.1.2 Higher order Godunov type scheme

The higher-order Godunov type method used for the computation in this section follows the MUSCL–Hancock method (see Toro, 1997). Let us introduce the extended variable

$$\mathbf{U} = \left(\mathbf{W}, a^1, a^2, a^3, b^1, b^2, b^3, c^1, c^2, c^3\right), \mathbf{F} = \left(\mathbf{H}, a^1u, a^2u, a^3u, b^1u, b^2, b^3u, c^1u, c^2u, c^3u\right),$$

$$\mathbf{K}_1 = (\mathbf{0}, 0, 0, 0, -b^1, -b^2, -b^3, -c^1, -c^2, -c^3), \mathbf{K}_2 = (\mathbf{0}, b^1, b^2, b^3, 0, 0, 0, 0, 0, 0).$$

The governing equations are written as

$$\frac{\partial \mathbf{U}}{\partial t} + \frac{\partial \mathbf{F}}{\partial x} + \mathbf{K}_1\frac{\partial u}{\partial x} + \mathbf{K}_2\frac{\partial v}{\partial x} = 0.$$

The flow variables are characterized by a mean value $\mathbf{U}_i^n$ and a slope $\delta\mathbf{U}_i^n$. The slopes are computed with conservatives variables but other options are possible. The conservative variables at the cell boundaries are given by $\mathbf{U}_{i+1/2,-}^n = \mathbf{U}_i^n + \frac{1}{2}\delta\mathbf{U}_i^n$ and $\mathbf{U}_{i-1/2,+}^n = \mathbf{U}_i^n - \frac{1}{2}\delta\mathbf{U}_i^n$. These boundary variables are then evolved over a half time step by:

$$\mathbf{U}_{i-1/2,+}^{n+1/2} = \mathbf{U}_{i-1/2,+}^n - \frac{1}{2}\frac{\Delta t}{\Delta x}\left(\mathbf{F}_{i+1/2,-}^n - \mathbf{F}_{i-1/2,+}^n\right)$$
$$-\frac{1}{2}\frac{\Delta t}{\Delta x}\left(u_{i+1/2,-}^n - u_{i-1/2,+}^n\right)(\mathbf{K}_1)_i^n - \frac{1}{2}\frac{\Delta t}{\Delta x}\left(v_{i+1/2,-}^n - v_{i-1/2,+}^n\right)(\mathbf{K}_2)_i^n,$$
$$\mathbf{U}_{i+1/2,-}^{n+1/2} = \mathbf{U}_{i+1/2,-}^n - \frac{1}{2}\frac{\Delta t}{\Delta x}\left(\mathbf{F}_{i+1/2,-}^n - \mathbf{F}_{i-1/2,+}^n\right)$$
$$-\frac{1}{2}\frac{\Delta t}{\Delta x}\left(u_{i+1/2,-}^n - u_{i-1/2,+}^n\right)(\mathbf{K}_1)_i^n - \frac{1}{2}\frac{\Delta t}{\Delta x}\left(v_{i+1/2,-}^n - v_{i-1/2,+}^n\right)(\mathbf{K}_2)_i^n.$$

Here the fluxes are defined as follows

$$\mathbf{F}_{i\pm1/2,\pm}^n = \mathbf{F}(\mathbf{W}_{i\pm1/2,\pm}^{n+1/2}).$$

The Riemann problem is then solved with the cell boundary states $\mathbf{U}_{i\pm1/2,-}^{n+1/2}$ on the left and $\mathbf{U}_{i\pm1/2,+}^{n+1/2}$ on the right as the initial data. The solution is then evolved over the time step by :

$$\begin{aligned}\mathbf{U}_i^{n+1} &= \mathbf{U}_i^n - \frac{\Delta t}{\Delta x}\left(\mathbf{F}^{HLLC}\left(\mathbf{U}_{i+1/2,-}^{n+1/2}, \mathbf{U}_{i+1/2,+}^{n+1/2}\right) - \mathbf{F}^{HLLC}\left(\mathbf{U}_{i-1/2,-}^{n+1/2}, \mathbf{U}_{i-1/2,+}^{n+1/2}\right)\right)\\ &-\frac{\Delta t}{\Delta x}\left(u^{HLLC}\left(\mathbf{U}_{i+1/2,-}^{n+1/2}, \mathbf{U}_{i+1/2,+}^{n+1/2}\right) - u^{HLLC}\left(\mathbf{U}_{i-1/2,-}^{n+1/2}, \mathbf{U}_{i-1/2,+}^{n+1/2}\right)\right)(\mathbf{K}_1)_i^{n+1/2}\\ &-\frac{\Delta t}{\Delta x}\left(v^{HLLC}\left(\mathbf{U}_{i+1/2,-}^{n+1/2}, \mathbf{U}_{i+1/2,+}^{n+1/2}\right) - v^{HLLC}\left(\mathbf{U}_{i-1/2,-}^{n+1/2}, \mathbf{U}_{i-1/2,+}^{n+1/2}\right)\right)(\mathbf{K}_2)_i^{n+1/2}\end{aligned}$$

with

$$\begin{aligned}(\mathbf{K}_1)_i^{n+1/2} &= \mathbf{K}_1\left(\frac{\mathbf{U}_{i-1/2,+}^{n+1/2} + \mathbf{U}_{i+1/2,-}^{n+1/2}}{2}\right),\\ (\mathbf{K}_2)_i^{n+1/2} &= \mathbf{K}_2\left(\frac{\mathbf{U}_{i-1/2,+}^{n+1/2} + \mathbf{U}_{i+1/2,-}^{n+1/2}}{2}\right).\end{aligned}$$

Results presented in Section 4 are obtained by using the Van Leer limiter (1979).

3.2 Relaxation step

For each cells, we want to solve the following equation:

$$\frac{\partial\mathbf{G}}{\partial t} = \frac{a}{\tau_{rel}}\mathbf{GS} \tag{19}$$

This is done in the following way.

3.2.1 Singular Value Decomposition

At the hyperbolic step we have calculated the cobasis $\mathbf{e}^\alpha$, $\alpha = 1, 2, 3$. Hence, we have the real deformation gradient $\left(\mathbf{F}^T\right)^{-1} = \left(\mathbf{e}^1, \mathbf{e}^2, \mathbf{e}^3\right) = \left(\hat{\mathbf{F}}^T\right)^{-1}$. Using a classical "singular value decomposition" procedure we can rewrite the matrix $\left(\mathbf{F}^T\right)^{-1} = \left(\mathbf{e}^1, \mathbf{e}^2, \mathbf{e}^3\right)$ under the following form : $\left(\mathbf{F}^T\right)^{-1} = \mathbf{VKU}^T$ where $\mathbf{U}$ and $\mathbf{V}$ are two orthogonal matrices and $\mathbf{K}$ is a diagonal matrix. The eigenvalues of $\mathbf{K}$ are singular values of $\left(\mathbf{F}^T\right)^{-1}$. This procedure is contained in the LAPACK libraries. Then $\mathbf{G} = \mathbf{F}^{-T}\mathbf{F}^{-1} = \mathbf{VK}^2\mathbf{V}^T$, $\mathbf{G} = \hat{\mathbf{G}}$. The eigenvalues of this Finger tensor calculated during the elastic step are initial conditions for the relaxation equation (9).

3.2.2 Calculating the relaxed stress

We will relax the cobasis equations using approximate relaxation equations (15)-(16) :

$$\frac{dS_\alpha}{dt} = -\frac{S_\alpha}{\tau_{rel}}.$$

An example of exact solution of (15)-(16) is given by (17). It determines, in particular, the final state $S_{\alpha f}$. The matrices $\mathbf{V}$ and $\mathbf{U}$ do not change during the relaxation process.

3.2.3 Determining new cobasis vectors

Solve with respect to $\beta_{\alpha f}$, $\alpha = 1, 3$, the following system of three algebraic equations :

$$S_{\alpha f} = -\mu\omega^{1/2}\left(\beta_{\alpha f}^2 - \beta_{\alpha f} - \frac{\beta_{1f}^2 - \beta_{1f} + \beta_{2f}^2 - \beta_{2f} + \beta_{3f}^2 - \beta_{3f}}{3}\right) \tag{20}$$

where

$$\omega^{1/2} = \frac{\rho}{\rho_0} = const, \quad \omega = \kappa_1\kappa_2\kappa_3$$

and

$$\beta_{1f}\beta_{2f}\beta_{3f} = 1 \tag{21}$$

This system can be efficiently solved by a classical Newton-Raphson procedure. The three equations (20) are not independent, the solution will be given using the first two equations of (20) and equation (21).

Then, we calculate

$$\kappa_{\alpha f} = \omega^{1/3}\beta_{\alpha f}$$

When $\kappa_{\alpha f}$ are computed, the curvilinear cobasis $(\mathbf{e}^\alpha)_f$ can be updated using the singular value decomposition $\left(\mathbf{F}^T\right)_f^{-1} = \mathbf{V}\mathbf{K}_f\mathbf{U}^T$, where

$$\mathbf{K}_f = \begin{pmatrix} k_{1f} & 0 & 0 \\ 0 & k_{2f} & 0 \\ 0 & 0 & k_{3f} \end{pmatrix}, \quad k_{\alpha f} = \sqrt{\kappa_{\alpha f}}, \quad \alpha = 1, 2, 3.$$

We underline that the matrices matrices $\mathbf{U}$ and $\mathbf{V}$ do not change during the relaxation step.

3.3 Summary

The numerical method can be summarized as follows:

- At each cell boundary the Riemann problem without relaxation terms is solved. The HLLC is recommended due to its simplicity, robustness and accuracy.
- Evolve all flow variables with the Godunov type method.
- Decompose the matrix$\left(\mathbf{F}^T\right)^{-1} = \left(\mathbf{e}^1, \mathbf{e}^2, \mathbf{e}^3\right)$ using the "singular value decomposition" .
- Compute the relaxed stress tensor.
- Determine the relaxed deformations.
- Update the cobasis vectors.

4 Numerical results

In the all numerical experiments of this Section, we consider steel with the following parameters: $\rho = 7850kg/m^3$, $\gamma = 2.84$, $p_\infty = 6.\,10^8 Pa$, $\mu = 77\,GPa$, $Y = 2.49\,GPa$ (Kluth & Despres, 2008). In all these tests, the CFL is 0.7 (calculated with respect to the velocity of longitudinal waves).

4.1 Impact test problem with shear

In this test, we have two steel plates impacting at $400m/s$ with a transverse velocity jump of 400m/s. Initially, the materials are at pressure $p = 0.1MPa$, initial density $\rho = 7850kg/m^3$ and zero initial shear stress. Impacts of the two materials occurs at $x = 0.5m$.

Figure 2 represent the numerical solution at time $t = 0.1ms$ for different meshes: 100 (square), 1000 (line), 5000 (dot line). This test show the convergence of the method for the shear impact test case.

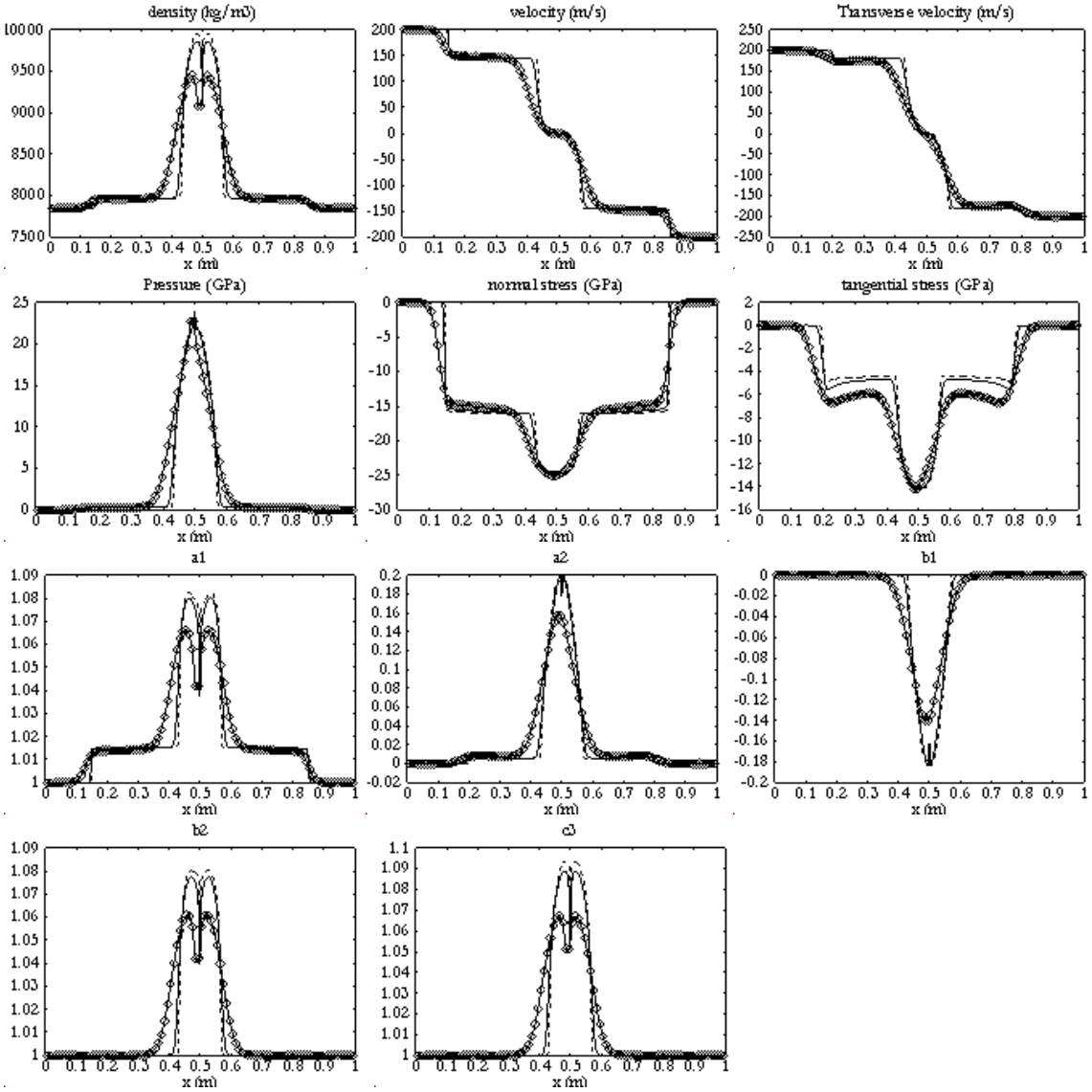

Figure 2: Impact test problem with shear, the output is shown at time $t = 0.1ms$ for different meshes: 100 cells (square), 1000 cells (line), 5000 cells (dotline). This test shows the convergence of the method.

4.2 Low yield limit

Consider the case where the yield limit is very small : $Y = 2.49 \times 10^{-9}Pa$. The other material parameters are the same : $\mu = 77\,GPa$ etc. Initially, a transverse speed discontinuity of 100 m/s

is imposed at $x = 0.5m$. Numerical results for a 1000 cells mesh are shown in Figure 3 at time $t = 0.1ms$. The tangential speed is diffused. A negligibly small amount of shear stress is created ($\sim$0.02 Pa). An overshoot due to the kinetic energy averaging is present. This test shows the capability of the method to deal with sliding.

4.3 Relaxation test

In this test, we consider an immobile rigid wall on the right, and on the left we consider a piston moving at constant velocity of $-1m/s$ during $150ms$ ($0 \to 2$) then we stop ($2 \to 3$). The relaxation time τ_{rel} is :

$$\frac{1}{\tau_{rel}} = \frac{1}{\tau_0}\left(\frac{Min\left(\sum_\alpha S_\alpha^2 - \frac{2}{3}Y_0^2, 0\right)}{\frac{2}{3}Y_0^2}\right) + \frac{1}{\tau_1}\left(\frac{Min\left(\sum_\alpha S_\alpha^2 - \frac{2}{3}Y_1^2, 0\right)}{\frac{2}{3}Y_1^2}\right)$$

with $\tau_0 = 10^{-20}s$, $\tau_1 = 1s$, $Y_0 = 2.47GPa$, $Y_1 = 247MPa$. The experimental configuration is shown in Figure 4. This model can be schematized as shown in Figure 5. Since $\frac{t}{\tau_0} \approx 10^{15}$, the relaxation to the yield surface determined by Y_0 is stiff. Y_1 corresponds to a residual stress, and τ_1 is the time to reach this limit. Results of numerical experiment are presented in Figure 6. During the loading step, the stress increases while the material stays in the elastic domain ($0 \to 1$), then it stays constant during plastic loading ($1 \to 2$). When the loading is stopped, the material starts to relax to the second yield limit ($2 \to 3$). This "long term" relaxation happens in many materials such as concrete, metals... This example shows the ability of the model to deal with the relaxation phenomena.

All these examples show that the relaxation time is a very important material parameter. The material softening and hardening may be described by the relaxation time dependence on temperature and pressure.

5 Diffuse interface model

In Favrie et al.(2009), a diffuse interface model has been constructed for description of a fluid – elastic solid interaction. The dynamics of interfaces separating fluid and solid as well as the corresponding boundary conditions have been naturally included in such a formulation. An analogous "multiphase" formulation can also be derived for the interaction of elastic-plastic solids with an ideal fluid. A model derivation will be published in a forthcoming paper. However, we would like to illustrate the ability of such a "multiphase" formulation for the treatment of complex physical problems.

Let us consider an impact of a solid copper projectile on a solid copper plate. The initial configuration is shown in Figure 7. Such a problem has already been presented in Favrie *et al.* (2009). The projectile is a square of 0.1 m length and has an initial velocity of $800m/s$. The plate is of 0.5m length and 0.1m width. The other part of the domain contains air at atmospheric conditions. The domain is 0.7m long and 0.7 m high. The mesh contains 1000 cells in x and y directions. The air is considered as an ideal gas with $\gamma_g = 1.4$ The parameters of copper for the hydrodynamic part of the energy are : $\gamma_s = 4.22$, $p_\infty = 34.2GPa$, $\rho_s = 8900kg/m^3$. For the elastic part of the energy, we take $\mu = 92GPa$ and $Y = 2.49GPa$. In Figure 8, we compare the results for three time instants in three cases:

- the copper is considered as a fluid with $\mu = 0$ (on the left)
- the copper is considered as an elastic solid with $Y = \infty$ (in the middle)
- the copper is considered as a real elastic-plastic solid with realistic parameters (on the right)

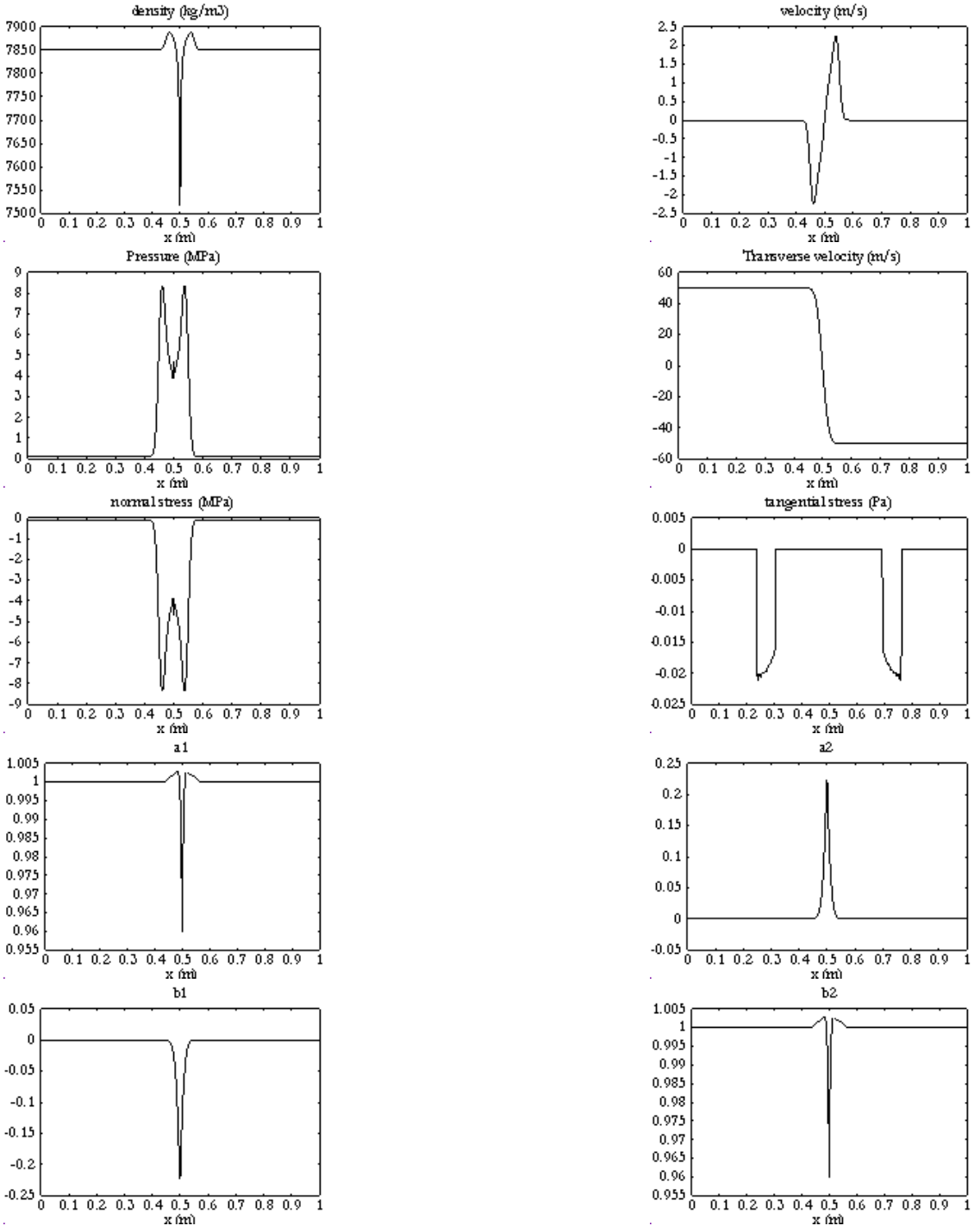

Figure 3: Low yield limit experiment. A transverse velocity jump is imposed initially in an elastic material with a very small yield limit. Solution is presented at time t=0.1ms. We notice the diffusion of a transverse velocity, a very low tangential stress is created ($\sim 0.02Pa$). This example shows the capability of the method to deal with sliding.

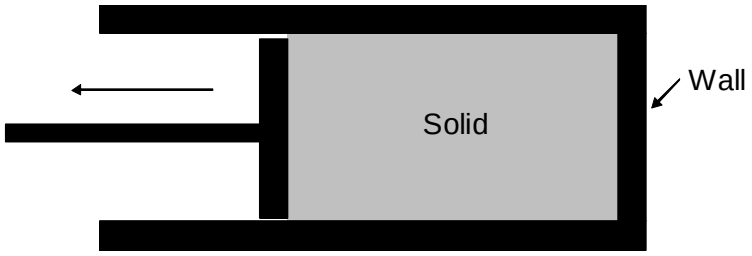

Figure 4: Geometrical configuration of the loading-unloading experiment.

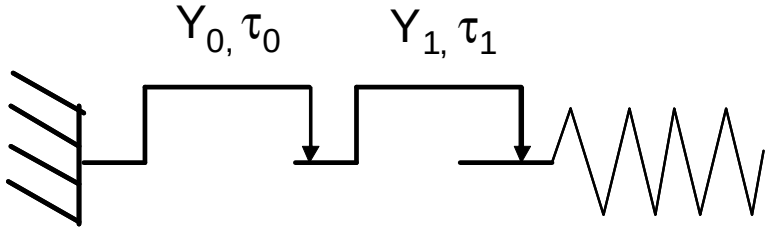

Figure 5: Schematic representation of the relaxation time with two yield limits $Y_1 < Y_0$, and the relaxation times $\tau_1 >> \tau_0$. The yield limit Y_0 is rapidly attained, and then slowly, it is decreasing to reach the value Y_1.

At initial time instant, a small amount of air ($\alpha_g = 10^{-4}$) is present in the solid. The presence of air allows to observe shock induced void nucleation and appearance of new interfaces (cracks) in solids.

Acknowledgments The authors thank Richard Saurel and Pierre Suquet for fruitful discussions. N.F. has been largely benefited from the discussion with Professor S. K. Godunov and Dr. I. Peshkov during his post-doctoral study at Sobolev Institute of Mathematics, Novosibirsk. The authors have been partially supported by grant N 07.34.048 from the DGA.

6 References

Barton, P.T., Drikakis, D. and Romenski, E. I. (2010) An Eulerian scheme for large elastoplastic deformations in solids, Int. J. Numer.Meth. Engng, **81**, 453-484.

Bertram A. (2005), Elasticity and Plasticity of Large Deformations. Springer-Verlag

Favrie and Gavrilyuk (2010) Mathematical and numerical model for nonlinear viscoplasticity, Philosophical Transactions of the Royal Society A -Mathematical Physical and Engineering Sciences (submitted).

Favrie, N., Gavrilyuk, S.L. and Saurel, R. (2009) Diffuse solid-fluid interface model in cases of extreme deformations, Journal of Computational Physics, **228**, 6037-6077.

Gavrilyuk, S.L., Favrie, N. and Saurel, R. (2008) Modeling wave dynamics of compressible elastic materials. Journal of Computational Physics, **227**, 2941-2969.

Germain, P. and Lee, E. H. (1973) On shock waves in elastic-plastic solids, J. Mech. Phys. Solids, **21**, p. 359-382.

Godunov, S.K., Denisenko, V.V., Kozin, N.S. and Kuz'min, N.K. (1975) Use of relaxation viscoelastic model in calculating uniaxial homogeneous strains and refining the interpolation equations for Maxwellian viscosity, J. Applied Mechanics and Technical Physics, **16**, N 5, 811-814.

Godunov, S.K. (1978) Elements of Continuum Mechanics, Nauka, Moscow (in Russian).

Godunov, S.K. and Romenskii, E.I. (2003) Elements of Continuum Mechanics and Conservation Laws, Kluwer Academic Plenum Publishers, NY.

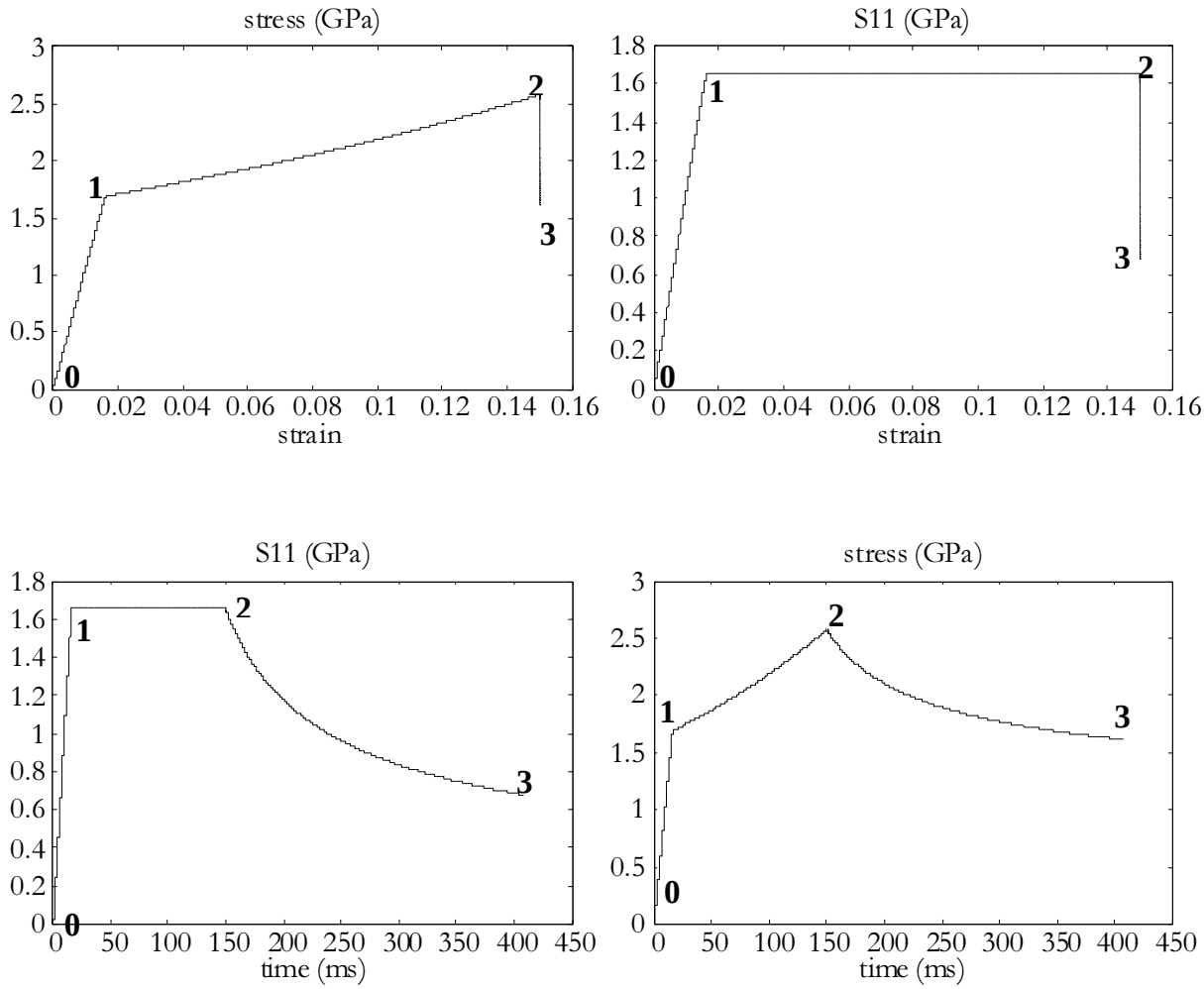

Figure 6: Relaxation test: A load is applied to the material. Then the deformation stays constant and long term relaxation appears. This test case highlights the possibility of the method to deal with time dependent phenomena.

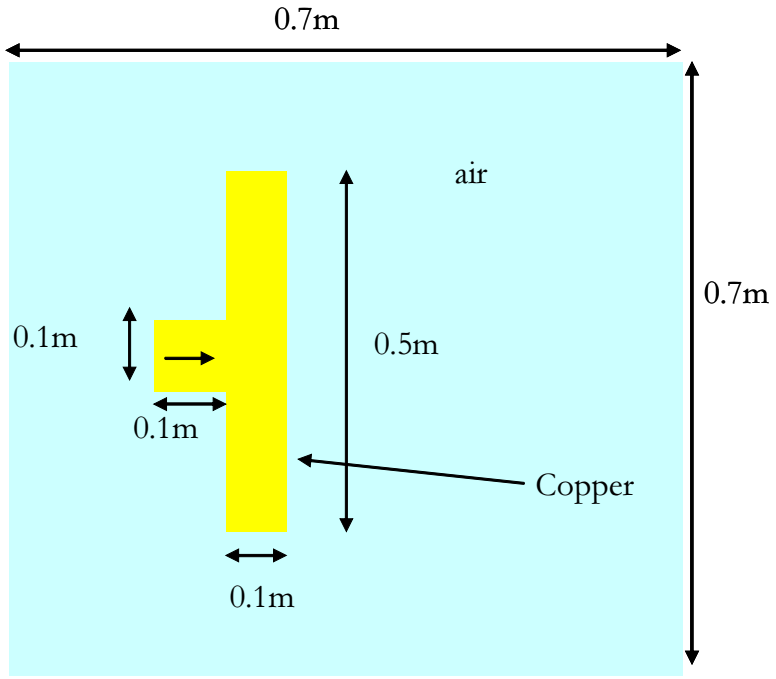

Figure 7: Initial configuration for the copper impact test problem: a square projectile of 0.1m length impacts a copper plate of 0.5m length and 0.1 m width at $800m/s$

Godunov, S. K. and Peshkov, I. M. (2010) Thermodynamically compatible nonlinear elasto-plastic model of Maxwell's continua, Computational Mathematics and Mathematical Physics (to appear).

Gouin, H. and Debieve, J.F. (1986) Variational principle involving the stress tensor in elasto-dynamics, Int. J. Engng. Sci., **24**, N 7, 1057-1066.

Kluth, G. and Despres, B. (2008) Perfect plasticity and hyperelastic models for isotropic materials, Continuum Mechanics and Thermodynamics, **20**, N 3, 173-192.

Lemaitre, J. and Chaboche, J. - L. (1988) Mécanique des matérieux solides, Dunod.

Miller, G.H., Colella, P. (2001) A high order Eulerian Godunov method for elastic plastic flow in solids Journal of Computational physics, **167**, 131-176.

Plohr, J. N. and Plohr, B. J. (2005) Linearized analysis of Richtmyer-Meshkov flow for elastic materials, Journal Fluid Mech., **537**, 55-89.

Simo, J. C. and Hughes, T. J. R. (1998) Computational Inelasticity, Mechanics and Materials, Interdisciplinary Applied Mathematics, v. 7, Edition Springer Verlag, New York.

Toro, E. F. (1997) Riemann Solvers and Numerical Methods for Fluid Dynamics, Springer.

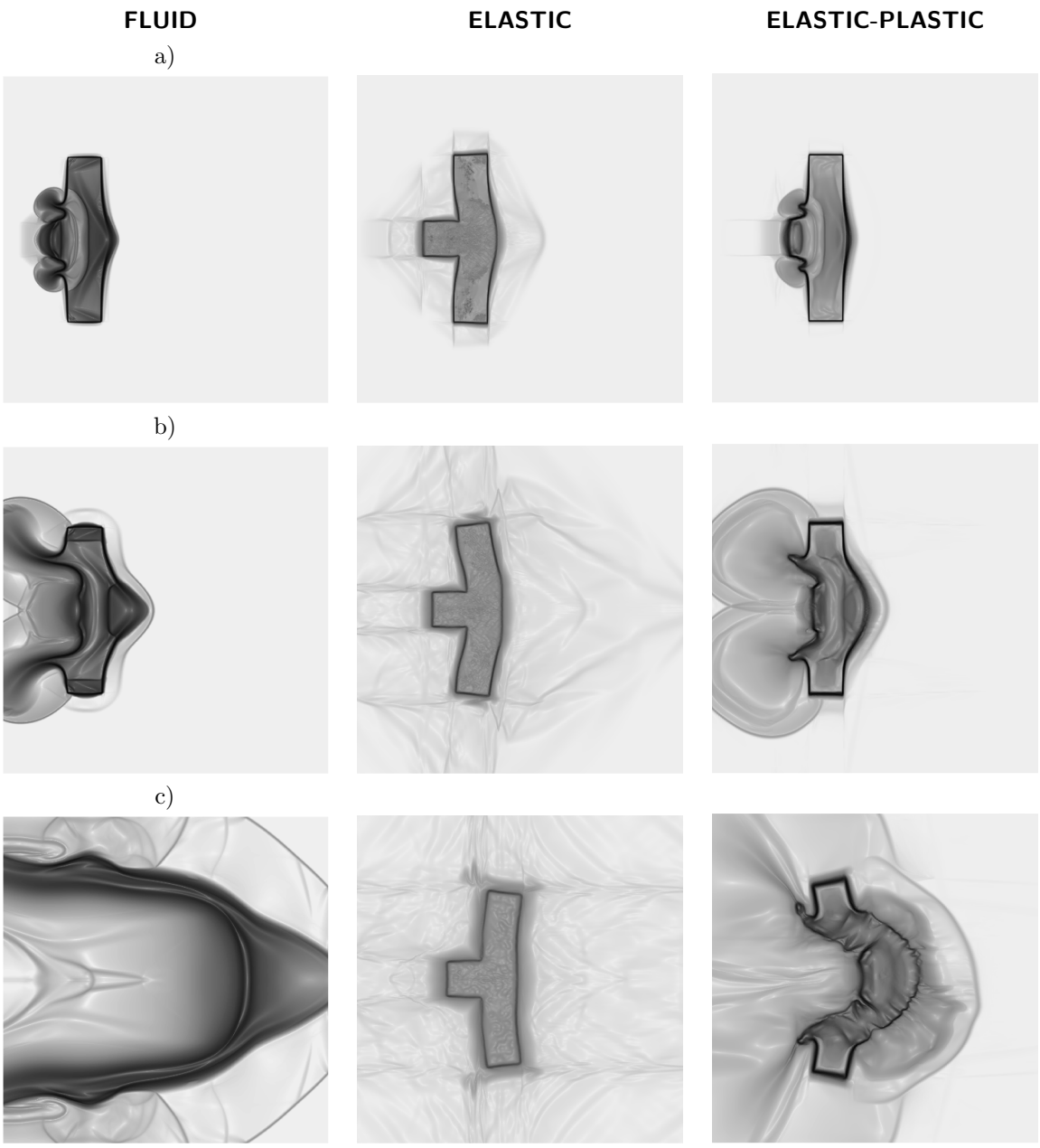

Figure 8: Impact at 800m/s of a copper projectile on a copper plate at rest surrounded by air at atmospheric pressure. The schlieren image of the density is shown for different time instants. Numerical computations involve 1000×1000 cells. In the fluid case (on the left, the time instants are $t = 100\mu s$, $t = 250\mu s$, $t = 1ms$) filaments appear and propagate to infinity, the strain being unbounded. In the elastic solid case (in the middle, the time instants are $t = 100\mu s$, $t = 300\mu s$, $t = 600\mu s$) the plate is really bent and oscillates. In the elastic-plastic case (on the right) more complex phenomena are present. At the first time instant (a)($t = 100\mu s$) the material shape is the same as for the fluid. The projectile is strongly bent and filaments start to appear. But as we can notice in Figure b the elasticity of the material will stop the extension of the filaments ($t = 250\mu s$). Figure c shows that after some time ($t = 600\mu s$) cracks start to appear in the elastic-plastic solid. This crack's formation is linked to the air nucleation in the copper. The filaments continue to break and multiple cracks start to appear in the plate. The extreme parts of the plate stay elastic and are not bent.